ORIGINAL RESEARCH

Modeling and experimental validation of the surface residual stresses induced by deep rolling and presetting of a torsion bar

Jasenko Perenda · Jovan Trajkovski · Andrej Žerovnik · Ivan Prebil

Abstract During the production of torsion bars, two different mechanical processes of inducing the residual stresses into the torsion bar are used: the presetting of the torsion bar and the deep rolling of the torsion bar. The process of presetting the torsion bar is carried out by twisting the torsion bar to the desired angle and releasing it to the new residual angle position. With controlled overstraining, favorable residual shear stresses are induced into the torsion bar, so the material is strain hardened and the yield point of the material is shifted and increased in the stress and strain space. The objective of the deep rolling process is to introduce compressive residual stresses into near-surface regions in order to increase the fatigue strength of the torsion bar. These two processes influence each other. The final level of residual stresses depends on the production sequence of these two processes and the production parameters of each process. The correct production sequence of these two operations and distribution of beneficial residual stress was simulated using the finite element (FE) method. To validate this model, the predicted surface residual stresses were compared by the X-ray diffraction (XRD) measurements of residual stresses.

J. Perenda (✉)
Sistemska tehnika d.o.o, Koroska c. 14, 2390 Ravne na
Koroskem, Slovenia
e-mail: jasenko.perenda@st-ravne.si

J. Trajkovski · A. Žerovnik · I. Prebil
Faculty of Mechanical Engineering, Chair of Modelling in
Engineering Sciences and Medicine, Askerceva c. 6,
1000 Ljubljana, Slovenia

J. Trajkovski
e-mail: jovan.trajkovski@fs.uni-lj.si

A. Žerovnik
e-mail: andrej.zerovnik@fs.uni-lj.si

I. Prebil
e-mail: ivan.prebil@fs.uni-lj.si

Introduction

Torsion bars are used in independent suspension system of high mobility tracked vehicles. This type of a suspension system consists of a torsion bar, road arm and road wheel. The road wheel is installed on the road arm, which rotates about the axis of the torsion bar as a result of the interaction between the road wheel and the ground. During the production process of torsion bars, two different processes of inducing the residual stresses into the torsion bar are used: the process of presetting and the deep rolling of the torsion bar. Presetting of the torsion bar is a process of repeated overloading of the torsion bar in the direction of normal service loads sufficient to develop a permanent set. This process is extensively used by spring makers and is known as presetting, prestressing, bulldozing and scragging [1]. Presetting results in an increase of the apparent yield stress and the endurance limit of the torsion bar. The process can be described as a treatment given to the torsion bar, the helical compression and other types of springs when they are loaded to such an extent as to produce yielding of the surface layers of the material [2]. In this respect, the process of presetting of the torsion bar is similar to the process of autofrettage of a thick walled tube. The presetting of the torsion bar is carried out by twisting the torsion bar to the desired angle and releasing it to the new residual angle position. At the maximum twist angle, the loading torque of the torsion bar reaches the maximum value and at the end of the release position, the loading torque of the torsion bar reaches the zero value. The torsion bar presetting method is recommended by the Society of Automotive Engineers (SAE). SAE recommends torsion bar presetting by twisting the torsion bar to the specified angle and releasing it for at least three times [3]. With the

process of controlled overstraining, favorable residual shear stresses are induced into the torsion bar. During the process of the presetting, the material is also strain hardened and the yield point of the material is increased. The strength of the torsion bar is increased because of a higher yield point of the material and induced residual stresses in the torsion bar [3]. Therefore, prestressed torsion bars can sustain higher service loads. Major drawback of this method is that the preset torsion bar can be loaded only in the direction of the overstraining.

The second process used during the torsion bar production is deep rolling. Deep rolling is a process of mechanical surface treatment which includes relative movement of a deep rolling tool – a roller. Beneficial effects of the mechanical surface treatments are mostly compressive residual stress profiles and strain hardening in near surface regions of components, yielding higher resistance against fatigue loading, corrosive environment or wear [4]. Some producers of torsion bars use the surface mechanical treatment process of shot peening. Schulze [5] showed that the residual stresses after deep rolling extend noticeably deeper into the interior of the material than the residual stresses do after shot peening.

Recommendations for production of torsion bars and production sequence of presetting and shot peening of torsion bars are presented in the SAE Manual on Design and Manufacture of Torsion Bar Springs [3]. The influence of shoot peening and presetting sequence on residual stresses was described by Almen [1]. Swift [6] presented a method for calculation of the residual stresses after presetting of torsion bars and the influence of the Bauschinger effect on the final level of residual stresses. The author also presented a successive layers removal method for measuring the residual stresses in a preset torsion bar. Calculation of torsional stresses based on the slopes from a torque-twist curve was presented by Fujczak [7].

Various authors implemented the FE method for calculation of residual stresses as a consequence of torsional loading. Kim [8] compared the results of FEM simulation with axisymmetric elements under torsional deformation with experimental results. He showed that Nadai's evaluation method, which is based on the assumption that the local shear strain is proportional to the distance from the axis, is reasonable. Brabie [9] analyzed the shearing stress distribution as a function of cross-section shape and dimensions for different twisted round bars. Rees [10] showed that the level of residual stresses that account for non-linear hardening behavior differ from simpler material models and are believed to be closer to the true distribution of residual stresses after torsional loading of a circular bar. Wang et al. [11] implemented an FE model of a loaded torsion bar for the calculation of the fatigue life of a torsion bar in high cyclic fatigue mode.

The process of deep rolling was studied by various authors. Skalski et al. [12] recognized the method of finite elements as an effective research tool in the analysis of contact strains. Guagliano and Vergani [13] researched the influence of the

deep rolling force on the evolution of residual stresses in notched components. Mayer [14] used an explicit Abaqus model to simulate the deep rolling process. The importance of the right material model and influence of kinematic hardening on residual stresses was published by Demurger et al. [15]. The simulation of residual stresses after deep rolling was based on non-linear kinematic hardening model. The simulation and the comparison of shoot peening with the deep rolling process was presented by Majzoobi et al. [16]. The authors used the Johnson-Cook constitutive material model. A combined isotropic/hardening model was implemented in FE simulation done by Bäcker et al. [17]. The authors examined the influence of different parameters of deep rolling on residual stresses. They presented deep rolling modeling with the coupled FE method and Boundary Element Method. Manouchehrifar and Alasvand [18] studied the influence of deep rolling parameters on residual stresses with FE simulation based on an explicit dynamic algorithm. Simulation of the deep rolling with an isotropic hardening material model based on Rastegaev type geometry compression tests was done by Balland et al. [19]. A combined isotropic and kinematic hardening model was used in FE simulation of deep rolling by Trauth et al. [20]. FE analysis of residual stresses after the deep rolling process, which is a part of manufacturing process, is presented by Werke [21]. The deep rolling process was recognized as the most critical part of the production sequence. FEM simulation of the manufacturing process and mapping of residual stresses after shot peening on a larger model with a complex surface was presented by Afazov [22].

The aim of deep rolling and presetting of the torsion bar is the same and that is to induce favorable residual stresses into the torsion bar. These two operations influence each other and the final level of residual stresses depends on the sequence of operations and process parameters of each operation as it will be shown through this article. The level of the residual stresses after presetting and deep rolling operations is influenced by many material and process parameters such as: cyclic properties of material, elasticity modulus change, Bauschinger effect, twist angle of presetting and deep rolling force. All these process parameters can be considered by the use of the FE modeling. However, this kind of FE simulations is very challenging and time costly. As shown through this survey, compressive residual stresses in the subsurface region will have a positive effect on the fatigue life of the torsion bar. Therefore, we would like to obtain the highest possible level of beneficial compressive residual stresses in subsurface regions, which can be achieved by a correct production sequence of the deep rolling and presetting operation. The sequence of these two operations is also influenced by possible obliteration of favorable residual stresses.

The aim of this article is to define a correct operation sequence of presetting and deep rolling in order to obtain the highest possible level of beneficial residual stresses in a torsion bar.

Theoretical basics of presetting and deep rolling

A short review of theoretical basics for the presetting operation is given in this chapter. Detailed information and equations can be found in the SAE manual HS-796 [3].

Presetting is an operation which increases the load capacity of the torsion bar in the direction of preset, but reduces it in the opposite direction. The operating torque must always be in the direction of the preset torque and should never be reversed [3]. Figure 1 shows the principle diagram of the torsion bar presetting.

The loading begins at point 0 and progresses to point I. There is a linear increase of torque with a windup angle. After point I, partial yielding occurs and the rate of torque buildup decreases up to the point II which represents the maximum specified torque. After removal of the load, the torsion bar returns from point II to point III elastically and along a straight line. In the figure, the distance 0-II shows a permanent set of the torsion bar. At point II, all the material in the bar is either in the yield range or below. Since the yield point is now at point II, any subsequent deflection from point III, for example to point IV, will be elastic. If the operating torque is lower than the presetting torque, the maximum load torque in service will correspond to a point such as point IV, and the yield point will not be reached again. The mechanism by which the bar produces the extra load carrying capacity is shown in Fig. 2. This graphical method for calculation of residual stresses was developed by G. B. Upton [3]. The method is similar to the Nadai's procedure for calculation of the residual stresses distribution from the torque-twist curve [7].

The curve 0-I-II is identical with the curve in Fig. 1, but the coordinates have been changed to stress versus strain. Strain ϒ, shown along the abscissa, is determined from:

$$\gamma = \theta d / 2L \qquad (1)$$

Nominal stress, shown along the ordinate, is derived from:

$$\sigma_3 = 16T / \pi d^3 \qquad (2)$$

This stress has no physical significance above point I, because it is calculated by a formula which is true only when Hooke's law holds. Actual stress at the surface can be derived from curve 0-I-II [3].

Tangent curve I-II intersects the y axis at point B. At the distance equal to ¼ OB, lies point C. The actual stress at the surface is equal to distance DC, when the nominal stress equals DA and strain equals 0D. Curve I-V is drawn by connecting a number of points found in this way and is the actual stress–strain curve for a point at the surface of the torsion bar. A linear scale is also shown along the abscissa with maximum strain 0E equal to unity. The assumption is that during the twisting of a circular bar, the cross sections remain plain and undistorted, so that the strain at any point is proportional to the radius. Therefore, at full preset, when the surface is at strain E, a point at 0.6 radiuses is under a strain of 0.6 times 0E and its stress is shown by the point of curve I-V above that abscissa. Curve 0-I-V shows the actual stress under full preset windup plotted against the radius. Linear stress distribution would give stresses along the straight line 0-V,
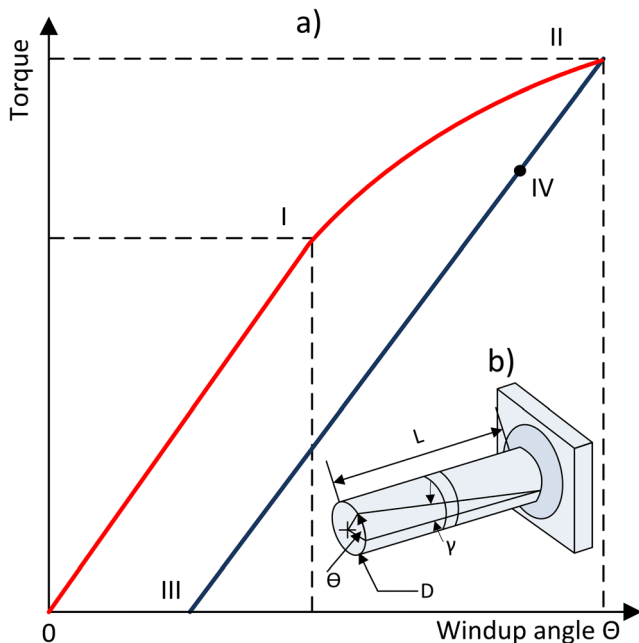

Fig. 1 Principle diagram of the torsion bar presetting
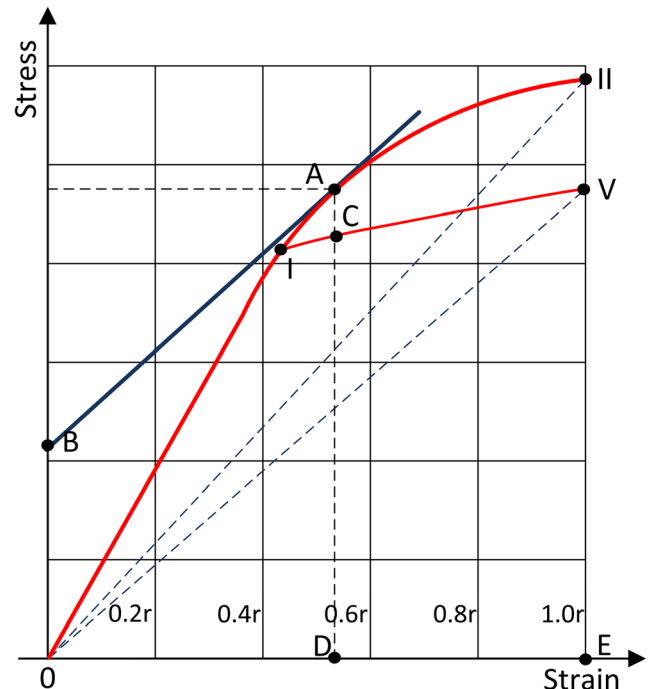

Fig. 2 Stress strain diagram during presetting

and the excess of stresses above this line accounts for the increase in stored energy.

The ordinate E-II shows the nominal stress at the surface when the bar is at full preset windup. When the bar is released, the nominal stress becomes zero, and the actual stress will be reduced by stress E-II. The residual stress equals to the difference between E-II and E-V. Similar reasoning applied to points below the surface shows that the residual stress at any radius is indicated by the difference between curve 0-I-V and the straight line 0-II. Residual stresses are the major reason for increased load capacity of the torsion bar.

One of the well-known benefits of deep rolling as compared to other surface treatments is the great depth of the strain hardened layer and compressive residual stresses. Another one is the generation of a glossy surface with low roughness as compared to treatments such as shot peening. These three effects can significantly enhance the mechanical behavior of metallic materials, especially under cyclic loading [23].

Deep rolling induces residual stresses in the surface layer of the workpiece. Maximum equivalent stresses are bellow surface as expected by Hertzian theory. Position of maximum residual stress depends on the rolling force and on the exact contact geometry of the workpiece and the tool as observed by Klocke et al. [24]. For example, with an increasing rolling force compressive residual stresses increase until they saturate at the level determined by the yield strength of the material. In very hard material states (e.g., case-hardened steel), near-surface work softening by deep rolling can be observed as noted by Altenberger [23] and Klocke et al. [25]. The substantial disadvantage of deep rolling is the complex determination of suitable process parameters. Because many parameters influence the level of residual stresses, the best way to determine residual stresses after the deep rolling operation is to use FE simulation [20]. FE modeling of the deep rolling operation is explained in the section about FE modeling of the production sequence.

Experimental setup

A specific production sequence of torsion bars consists of the deep rolling process before the presetting operation. To evaluate the mutual influence of these two operations on the value of residual stresses, an opposite combination of presetting before deep rolling was implemented. The additional combination of the examined production sequence consists of the first presetting, deep rolling of the torsion bar and the second presetting of the torsion bar, as presented in Table 1.

Residual stresses were measured on 12 torsion bars. Sample torsion bars were randomly taken from a batch of three different types of torsion bars from serial production, which differ in length and diameter of the torsion bar. Major dimensions and average values of presetting angles of investigated torsion bars differ, but the value of the final elastic shear strain calculated according to the Eq. 1 is the same (0.0192). Residual stresses were measured at six points on the surface of the torsion bar as shown in Fig. 3, after completion of a specific production operation in the production sequence.

The measuring points were positioned as opposite pairs at the middle and at the both ends of the torsion bar. Residual stresses were measured with the XRD device Xstress 3000 G2R and $\sin^2\psi$ method with CrKa radiation. The ψ angle varied between $-45°$ and $+45°$ with six inclinations per side (12 angles in total). Residual stresses were measured with a 3 mm collimator.

The investigated sample torsion bars were made of TORKA-ESR steel (Metal Ravne designation). This type of steel is used for serial production of torsion bars. TORKA steel was specially developed for this kind of application. Nominal chemical composition of the steel is given in Table 2. AISI 4340 has a similar chemical composition.

Sample torsion bars were quenched prior to polishing, presetting and deep rolling. The presetting and deep rolling operations were conducted on the purpose-built machines (Fig. 4).

The presetting operation was controlled by a specified torque and twist angle of the torsion bar. The presetting operation was done by repeatedly twisting the torsion bar to the prescribed angle. Averaged values of the measured torque-twist curves of the torsion bars (Type I and Type II) are given in (Fig. 5).

The specimens were deep rolled using a purpose-built machine. Three rollers (diameter 80 mm, hardness 64 HRC), hydraulically controlled, are placed at a 120 degree angle around the workpiece (Fig. 4). The process of deep rolling is done in three steps. First, rollers are pressed against the rotating torsion bar. When the requested pressure (40 bar) is reached, a carriage with rollers starts to move in the axial direction with a specified feed rate (1.5 mm/s). At the end of the deep rolled area, rollers are moved away from the torsion bar. During the deep rolling, the torsion bar is cooled and oiled with a highly refined mineral oil. The deep rolling force is

Table 1 Major dimensions and production parameters of the investigated torsion bars

	Diameter (mm)	Active length (mm)	Deep rolling force (N)	Feed rate (mm/s)	Presetting angles / residual angles (deg)	Production sequence
Type I	39.3	1230.1	11700	1.5	157 / 88.1	Deep rolling Presetting
Type II	44.2	1456.2	11700	1.5	163 / 90.4	Deep rolling Presetting
Type III	54.7	1978.6	11700	1.5	140 / 64.6 99 / 19.4	Presetting Deep rolling Presetting

Fig. 3 Position of measuring points of residual stresses
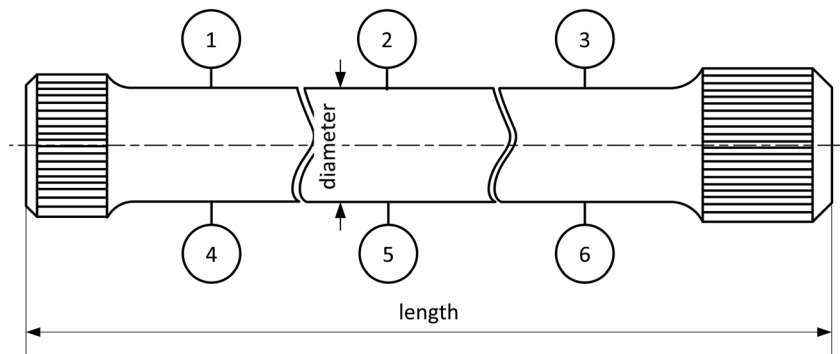
calculated from the pressure in roller cylinders (Table 1). The feed rate of deep rolling was recorded from the machine and controlled with measurement of the distance through time.

Material characterization

As stated before, simulated residual stresses of a solid circular bar in torsion with the use of non-linear hardening material behavior differ from simpler material models and are closer to the true distribution of residual stresses, Rees [10]. Also good agreement between simulated and measured residual stresses after the deep rolling operation was achieved with the use of a non-linear combined hardening model as shown by Trauth et al. [20]. Therefore, in this work the Lemaitre-Chaboche material model [26] is used to describe the cyclic behavior of the investigated material through the presetting and deep rolling operation. The model represents superposition of a non-linear kinematic hardening component. The kinematic hardening component describes the translation of the yield surface in stress space through backstress. The isotropic hardening component describes the change of the equivalent stress with the size of the yield surface as a function of plastic strain. The following equations present only a review of basic equations used in the material model. Detailed derived equations are given in [27].

The isotropic hardening part of the equation corresponds to the uniform expansion of the initial criterion. The evolution of the isotropic component of the combined hardening rule is defined by the following equation:

$$dR = b(Q-R)dp \qquad (3)$$

where b and Q are two constants, given by the type of material. dR represents a change of size of the elastic domain, Q is

an asymptotic value which corresponds to a regime of stabilized cycles, b indicates the speed of stabilization and dp presents accumulation of plastic strain. The initial value of elastic domain may be taken as zero or nonzero $R(0)=R_0$. Integration of Eq. (3) results in:

$$R(p) = Q(1-e^{-op}) \qquad (4)$$

The kinematic part of the non-linear kinematic-isotropic hardening model is represented by evolution of a linear kinematic term and a recall term which introduce a fading memory effect of the strain path.

$$dX = \frac{2}{3}C(p)d\varepsilon^p - \gamma(p)Xdp \qquad (5)$$

In Eq. (5), dp is the increment of the accumulative plastic strain, and C and γ are the characteristic coefficients of the material. When the range of changes in strain is significant, it is better to use superposing of several analogous models represented in Eq. (5).

$$X = \sum_{i=o}^{n} X_i \qquad (6)$$

To obtain parameters of isotropic and kinematic hardening, a series of monotonic and cyclic experiments were conducted as described by Kunc and Prebil [28]. Specimens used for a series of cyclic tension compression tests were quenched and tempered together with the analyzed samples of torsion bars. Variable amplitude fatigue tests conducted in a fully reversed push pull control condition were carried out on INSTRON

Table 2 Chemical composition (in weight %) of Torka steel (Metal Ravne designation)

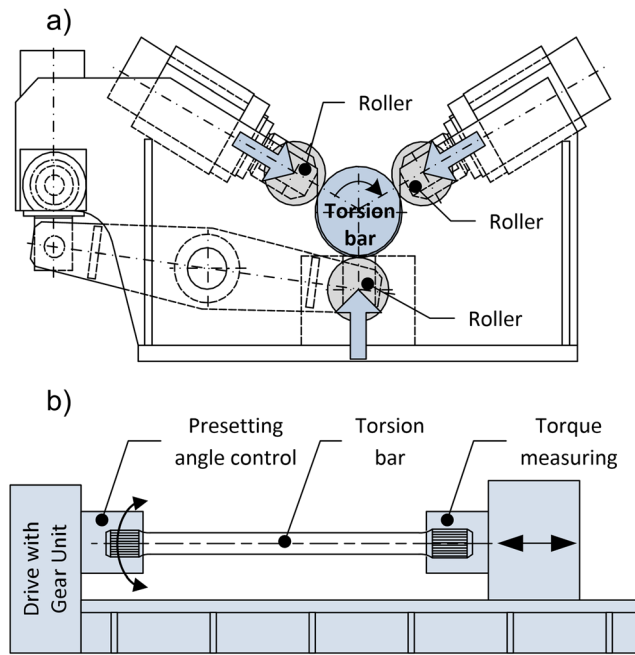|	C	Si	Mn	Ni	Cr	Mo	V	Cu	S	P
Min.	0.42 %	0.17 %	0.5 %	1.3 %	0.8 %	0.2 %	0.1 %	0 %	0 %	0 %
Max.	0.5 %	0.37 %	0.8 %	1.8 %	1.1 %	0.3 %	0.18 %	0.25 %	0.001 %	0.02 %

a)

b)

Fig. 4 **a**) Deep rolling machine **b**) Presetting machine

8802. The extensometer used for measurements was Instron Dynamic 2620–603 (gauge length 10 mm, full scale range ±1 mm). Controlled strain amplitudes were 0.7, 1, 1.5, 2, 2.5 and 3 %. A drawing of a tensile specimen is shown in Fig. 6. To avoid the buckling of the specimen at higher strains, the diameter of the tensile specimen was enlarged.

Variation of maximum and minimum stress values with a number of loading cycles, obtained by fully reversed cyclic loading, is shown in Fig. 7. It is evident that the chosen material is a cyclically softening material.
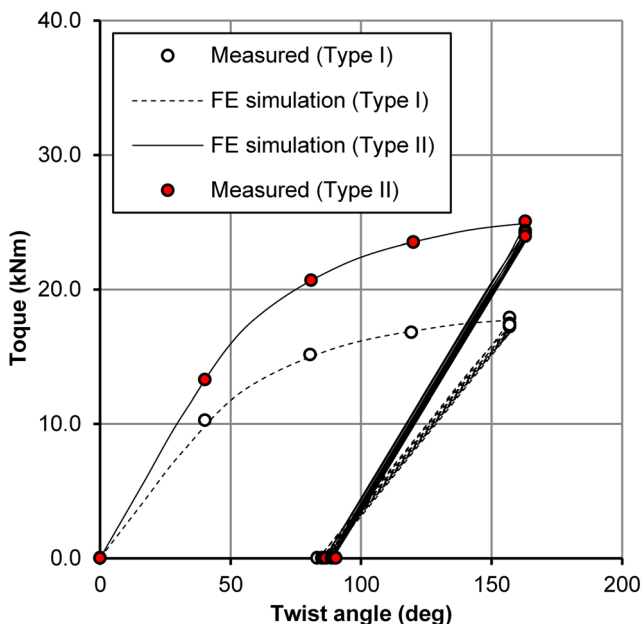
Fig. 5 Torque-twist curves (torsion bar Type I and Type II)

The described Lemaitre Chaboche-plasticity model was calibrated on a cyclically loaded FE model with one element as presented by Trauth et al. [20]. The model calibration is done by stress strain data from half-life hysteresis with the strain range of ±2 %. The results of model calibration for the whole range of cyclic tests are shown in Fig. 8.

It is noticeable that the elasticity modulus changes with the accumulated plastic strain. The major reasons for a decrease of the elasticity modulus after plastic deformation are the increase of residual stress and micro cracks, and the variation in the dislocation structure inside the workpiece [29]. Elasticity modulus variation is incorporated into the material model with the simple FORTRAN subroutine. The value of the elasticity modulus is updated by the change of the accumulated plastic strain and it is based on the measured values. Variation of the elasticity modulus is notable also from the pulsating tension test as shown in Fig. 9.

Figure 10 shows comparison of stress–strain curves of the pure tension test (dashed line), the pulsating tension test with controlled strain (dots) and the stress–strain curve of the simple FE model (one element). It is evident that the kinematic part of the combined material model has a major contribution to the change of the yield stress position and growth of the yield stress in the stress and strain space. With overstraining in one direction, the yield stress translates in the stress space and the resulted value of yield stress becomes larger. It is important to notice that the yield stress value is increased only in the direction of overstraining. In the opposite direction, the value of yield stress is smaller than the initial yield stress. This is the reason why the torsion bars can be loaded only in the direction of the presetting. Material model parameters obtained from model calibration as shown in Fig. 9 are presented in Table 3.

The material model obtained from the series of cyclic tests with values presented in Table 3 was verified with the torsion test of a torsion bar with specific dimensions (diameter 39.8 mm, length 1602 mm). The torsion bar was twisted for an angle of 320 degrees and released. Comparison of measured torque-twist curve and calculated torque- twist curve is shown in Fig. 10.

The FE model used in calculation of twist-torque curve presented in Fig. 10 is an axisymmetric model of the torsion bar. Details of FE modeling and boundary conditions are presented in the next chapter. The torsion bar preset with an initial twist angle of 320 degrees with markings for easier visualization of torsional deformation is shown on the right side of Fig. 10. Comparison shows very good correlation of measured and simulated results, so the combined material hardening model is appropriate for further modeling of the production sequence.

FE modeling of production sequence

The production sequence is simulated by two different combinations of presetting and deep rolling operations. In the first

Fig. 6 Drawing of specimens that were cycled on the INST RON 8802 machine
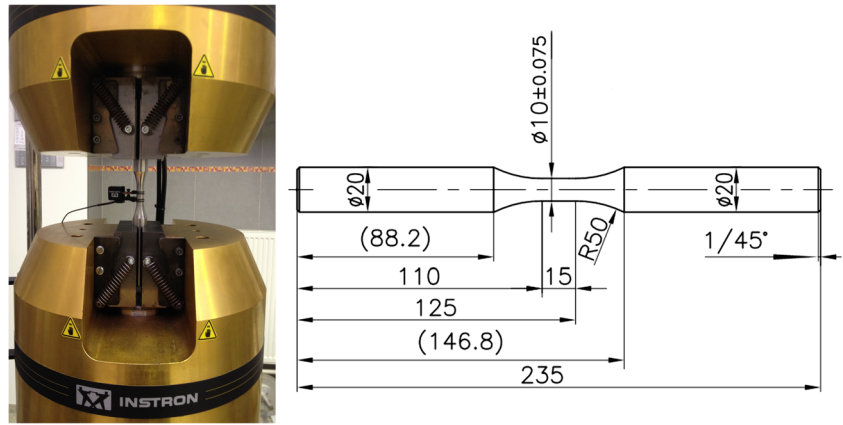
simulation, a production sequence consists of presetting and the deep rolling operation, whereas the second simulation of the production sequence is defined by the first presetting, deep rolling and the second presetting.

FE simulation of the presetting operation is straightforward. One can use axisymmetric [8] or 3D elements [30] for simulation of the torsional deformation and presetting operation. Due to the fact that the value of the twist angle depends on the length of a preset workpiece, it is possible to model only a cut-out of the whole workpiece geometry. Naturally, the twisting angle has to be reduced in relation to the whole length of the torsion bar-workpiece. To accurately model the overstraining and strain hardening effect of the torsion bar during the presetting operation, it is important to use a correct material model. As explained in the previous chapter, the kinematic part of the combined hardening model is used due to the fact that the yield surface will shift in the stress space, so

that the increased yield stress in one direction will reduce the yield stress in the opposite direction during the presetting. The isotropic part of the combined hardening model will have no major influence on the value of yield stress during the presetting operation, but it will influence the value of yield stress during the operation sequence of deep rolling. Torsion loading with twist angle control was completed by applying rotational displacement at one end of the model and fixed rigid boundary conditions at the other end of the model.

The deep rolling process simulation is more complex, because various process parameters influence the value of residual stresses after deep rolling. However, it is not necessary to model the entire work piece as the deep rolling process applies the same deformation across the entire surface layer. It affects only a layer the thickness of which is small as compared with the diameter of the part [19]. The process of deep rolling can
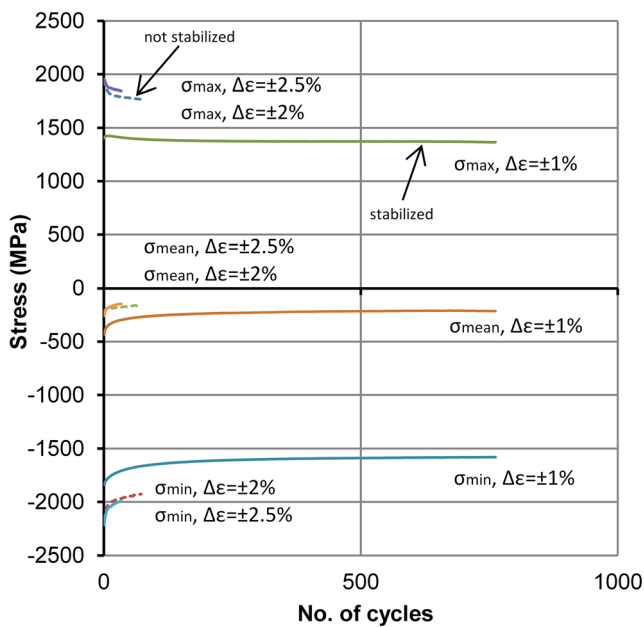

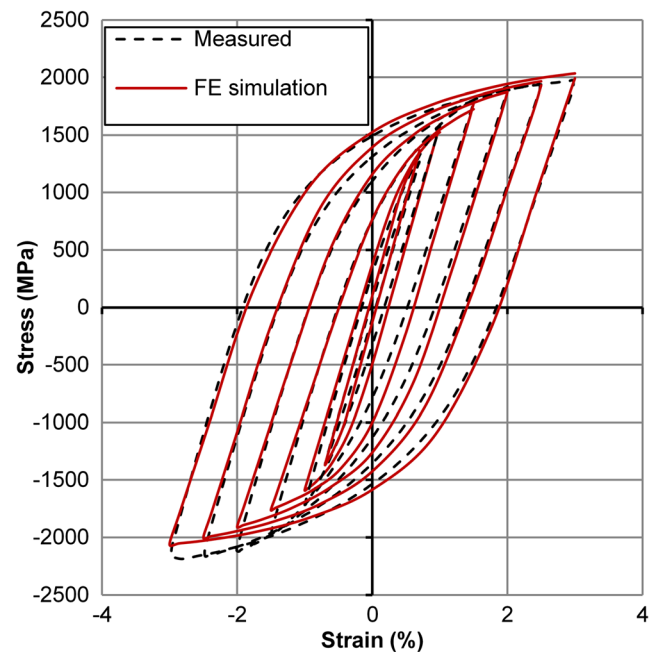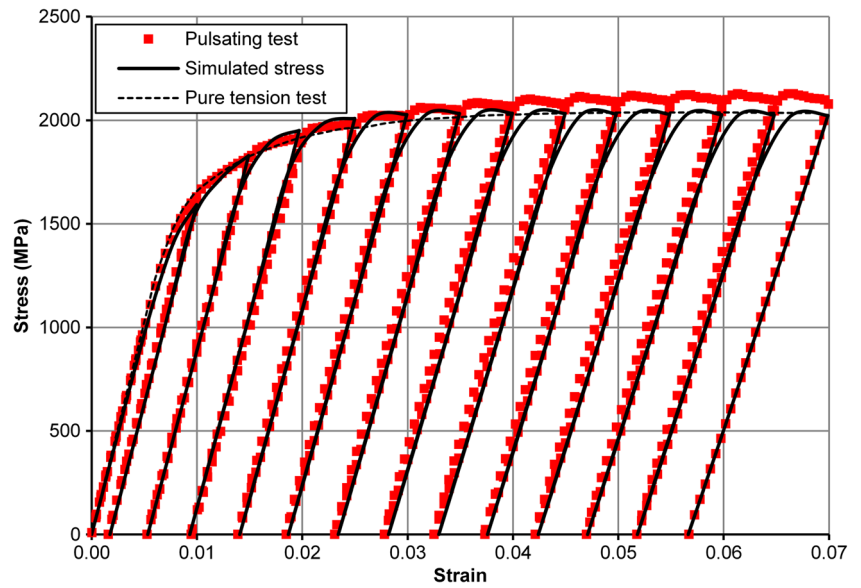**Fig. 7** Softening behavior of analyzed material at different strain amplitudes

Fig. 8 Comparison of stress strain response of the first loading cycle in the measured cycle and the FE simulation

Fig. 9 Calibration of the material model

be simulated as a quasi-static process. The explicit solver is more efficient in this type of problems and it is an appropriate choice for modeling three dimensional quasi static problems with nonlinear contacts such as the deep rolling process [20]. To simulate residual stresses after the deep rolling process, it is possible to represent a process with a small cut out of the symmetric specimen. To additionally decrease the computational time, a hole is added in a representative cut out model. The deep rolling process induces large strain gradients into the near surface region. To obtain accurate results, the mesh of the central part of the cut out has a higher density than unaffected regions with a coarse mash. The rolling force was calculated from the measurements of the rolling pressure (Table 1). The rotational speed of the roller is calculated from the rotational speed of the specimen. The axial movement of the rollers is simulated with multiple rollers which were initially displaced by the distance calculated from the feed rate and the rotational speed of the specimen (Table 1). The time for each rolling step is calculated from the rotational speed of the specimen. The contact is modeled with the master–slave contact algorithm and friction is modeled using the penalty method. The value of friction is 0.1. The dimensions of the observed volume with a fine mesh are 9 mm in the axial direction, 3 mm in the radial direction and 90 degrees in the circumferential direction. The mesh size in the middle changes with the depth. Dimensions of the mesh on the surface layer are $0.2 \times 0.3 \times 0.1$ mm. This portion of the cut-out with a high density mesh is the representative part for presenting simulation results. Boundary

Fig. 10 a) Comparison of the twist-torque curve of a real torsion bar and the FE simulation results **b)** torsion bar after presetting
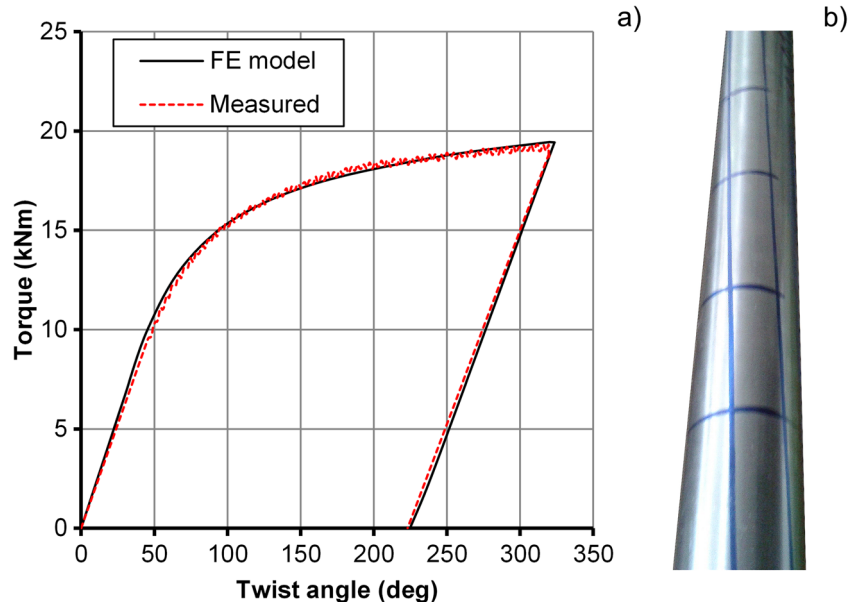
Table 3 Material model parameters obtained from model calibration

Parameter	σ_{yield}	E_{start}	ν	Q	b	C_1	Υ_1	C_2	Υ_2	C_3	Υ_3
Value	1020 MPa	201000 MPa	0.3	−220 MPa	2	251401	1135	35710	59	69739	269

conditions of the deep rolling simulation and averaged results of six nodal paths of deep rolling simulation are presented in Fig. 11.

FE simulations of production sequences were done with two different FE modeling approaches. The first modeling approach is based on the mapping of residual stresses after the deep rolling process on the axisymmetric model of the torsion bar. The major reason for using the mapping technique is to reduce the calculation time. In the first step of the production sequence simulation, simulation of the deep rolling process was done on a representative cut-out of the torsion bar. In the second step, an axisymmetric model was used for simulation of presetting the torsion bar with boundary conditions described in the introduction of this chapter. The axisymmetric model of a torsion bar is divided into the mapping regions. The size of the mapped regions is the same as the size of mesh elements used in the simulation of deep rolling process. The averaged result of residual stresses at six nodal paths after the deep rolling simulation is used for mapping the residual stresses onto the axisymmetric model. The initial step of the presetting simulation is an axisymmetric model of the torsion bar with mapped (predefined) stresses after deep rolling simulation. The comparison between the measured

and simulated torque-twist curve is given in Fig. 4. With this approach, it is possible to effectively simulate the production sequence of presetting after deep rolling (Fig. 12).

The second FE modeling approach is based on simulation of the deep rolling process and presetting operation on a representative 90 degree cut-out. As stated before, it is not necessary to model the whole torsion bar for the simulation of the deep rolling process or for the simulation of presetting. Obviously, we can expect lower torque values of the preset cut-out with a hole, because it has a smaller cross section area, but residual stresses at the surface of a cut out will be almost the same as the residual stresses of the 3D element model or axisymmetric model of the torsion bar. Because of the shorter calculation time during demanding simulation of the deep rolling process, this simplification is acceptable. During simulation of presetting, the representative cut-out is fixed at one end and loaded on the other for the value of the specified twist angle. Cyclic symmetry boundary conditions were applied on the flanks of the cut-out model. Results of the presetting analysis were used as initial stress–strain state for simulation of deep rolling. Results of this simulation were imported into additional simulation of the second presetting operation after deep rolling. The torque – twist curve of the simulated cut-out

Fig. 11 a) Deep rolling simulation setup; **b)** boundary conditions; **c)** averaged results of simulation
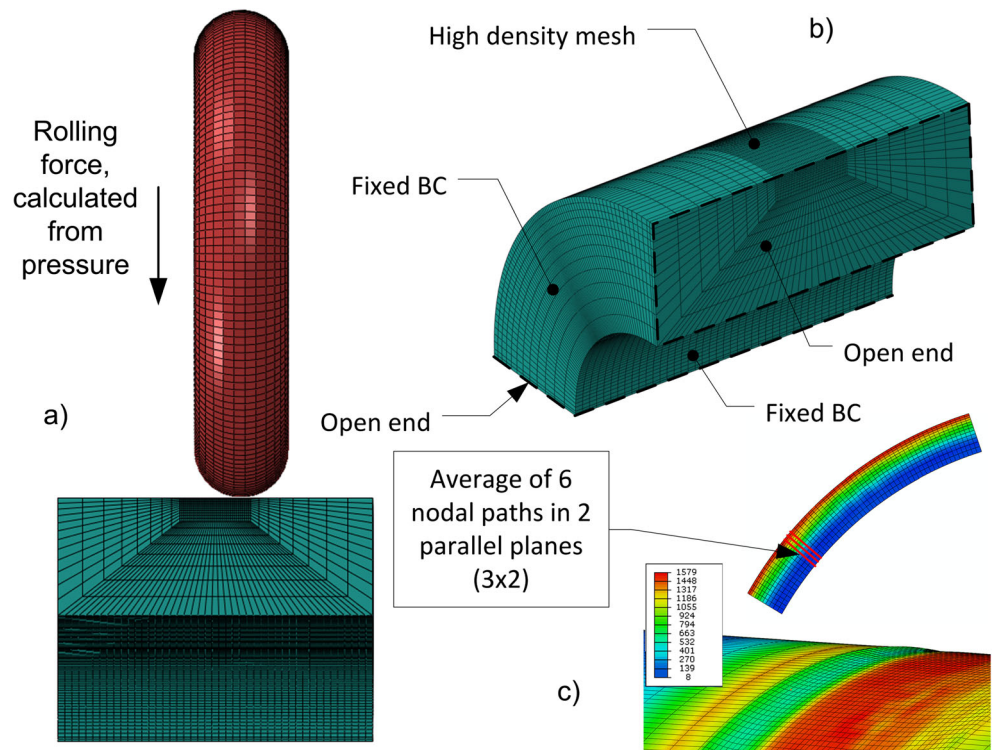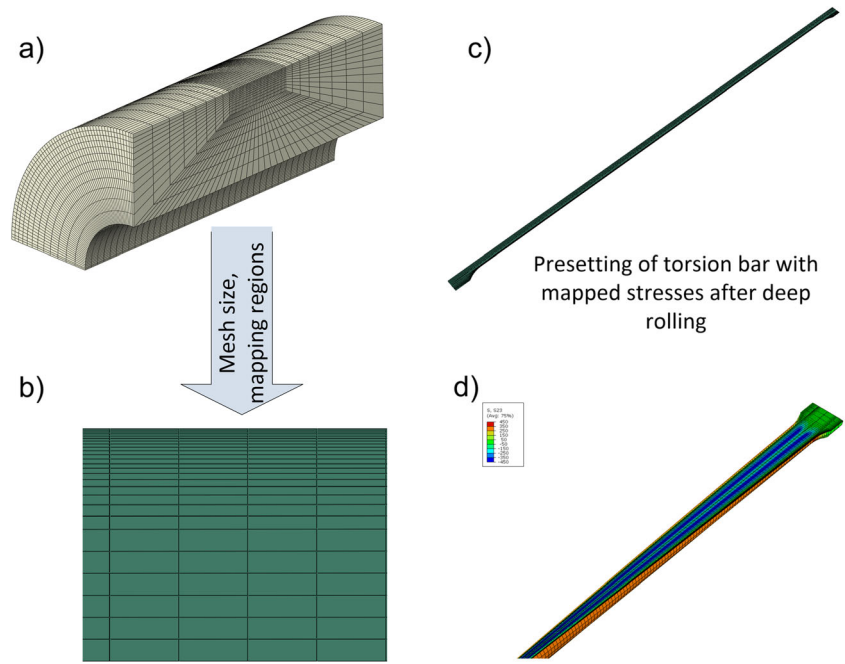
Fig. 12 **a**) Simulation of deep rolling with a cut-out; **b**) mapping of the values; **c**) presetting simulation - axisymmetric model **d**) results


model was compared to the measured torque-twist curve (Fig. 13)

The error of the predicted residual angle in both cases (axisymmetric model and cut-out model) after the first and second presetting is less than 2 degrees. Obviously, with simulation of the simplified cut-out model it is possible to obtain accurate results. Comparison of residual shear stresses after the first presetting of a representative cut out model, axisymmetric model of the entire torsion bar and full size 3D element model is given in Fig. 14. The measured residual stresses are presented in the following chapter.

To summarize this section: in both FE simulations of the production sequences (deep rolling - presetting and presetting I - deep rolling - presetting II), it is necessary to calculate the residual stresses after the deep rolling process on the 90° cut-out model. In order to reduce the calculation time, it is possible to use these results as predefined / input data for the axisymmetric model of the presetting operation. The production sequence of presetting before the deep rolling operation and additional presetting was simulated with the 90° cut-out model. The results of both simulations were validated with XRD measurements as presented in the next section.

Fig. 13 Comparison of the torque twist curve of axisymmetric model, cut-out model and measured values (*torsion bar* - Type III)
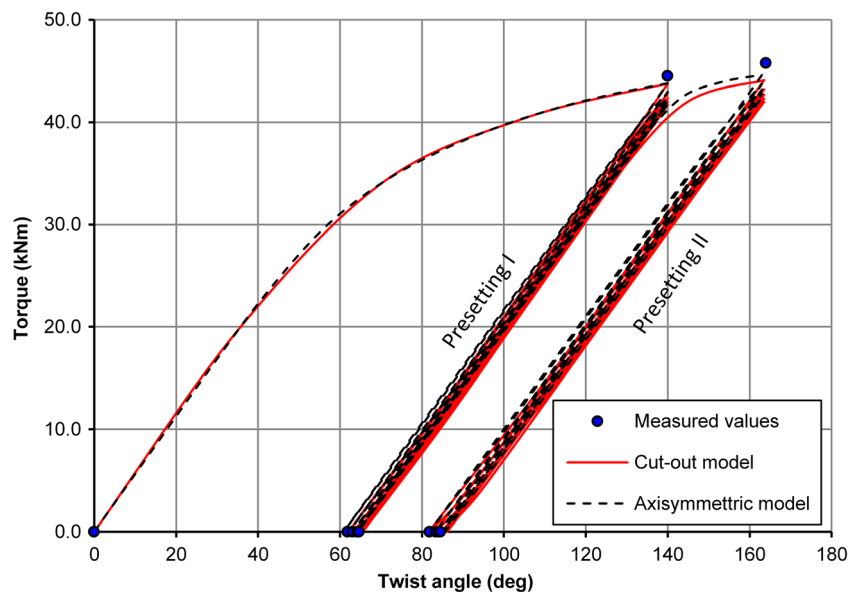
Validation of FE simulations and discussion

The accuracy of the presented FE models is verified by measurements of residual stress as described previously. Residual stresses were measured at the end of each production operation. Comparison of average measured values of residual stresses (torsion bar Type I and II) and results of the first FE simulation, the axisymmetric model of the preset torsion bar with mapped values of residual stresses after deep rolling, is given in Fig. 15.

It is notable that the presetting operation obliterated favorable residual stresses both in axial and circumferential direction from the deep rolling operation. The final value of residual stresses depends on technology parameters of deep rolling and presetting, but in any case axial and circumferential residual stresses will be lower after the presetting operation. Both measured and simulated results confirm this effect. Simulated results are in good agreement with the measured ones. The beneficial effect on fatigue life at ambient temperatures from the deep rolling processes can be ascribed to the creation of significant near-surface compressive residual stresses and a near-surface work hardened layer [31]. With the presetting operation after deep rolling, we reduce favorable residual stresses and in such way influence the fatigue life of the torsion bar. At the same time, with the presetting operation we induce residual shear stresses and increase the strength of the torsion bar. The profile of residual stresses after the deep
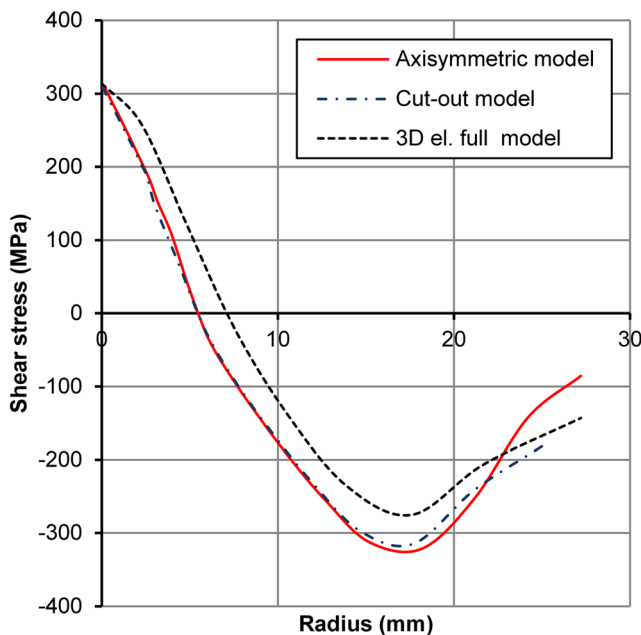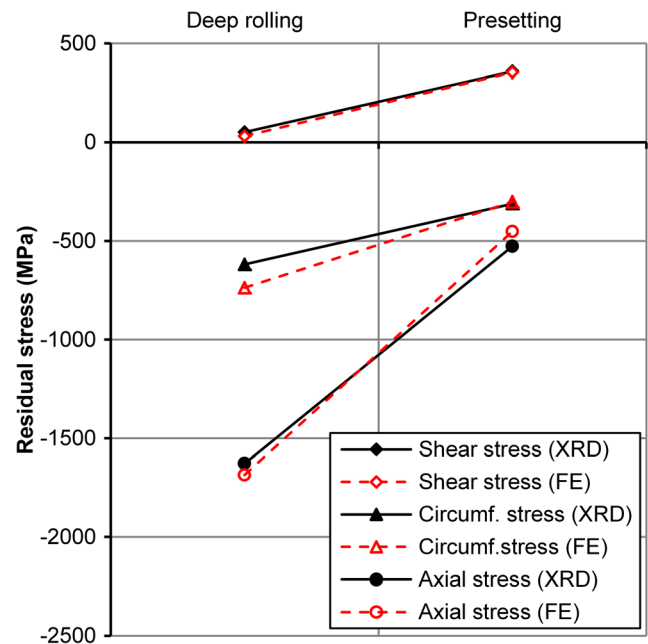

Fig. 15 Comparison of residual stresses after the deep rolling and presetting operation (*torsion bar* - Type I and II)

rolling and presetting operation, through the torsion bar depth, is given in Fig. 16.

As seen in Fig. 16, there are reduced residual stresses on the surface of the torsion bar after the deep rolling operation in axial and circumferential direction and induced shear stress. The question is what happens with residual stresses if the sequence of these two operations is switched. We can expect that the deep rolling operation will obliterate favorable shear stresses from the presetting operation, but at the end of deep rolling process there are going to be higher residual stresses in axial and circumferential direction. Figure 17 shows comparison between measured results (Type III torsion bar) and results of FE simulation (cut-out model) of the production sequence of presetting before the deep rolling operation.

Measured residual stresses in axial and circumferential direction after the first operation of presetting are induced by the polishing operation, which was not simulated. As can be seen from Fig. 17, there are induced shear stresses on the surface of the torsion bar after the first operation of presetting. Deep rolling obliterated favorable shear stresses at the surface. During torsional loading, the highest shear stresses are at the surface of the torsion bar and with obliteration of residual shear stresses, the load strength of the torsion bar is reduced. However, there are higher residual stresses in axial and circumferential direction. As stated before, these stresses have a major impact on fatigue life of the torsion bar. The profile of residual stresses through the depth after
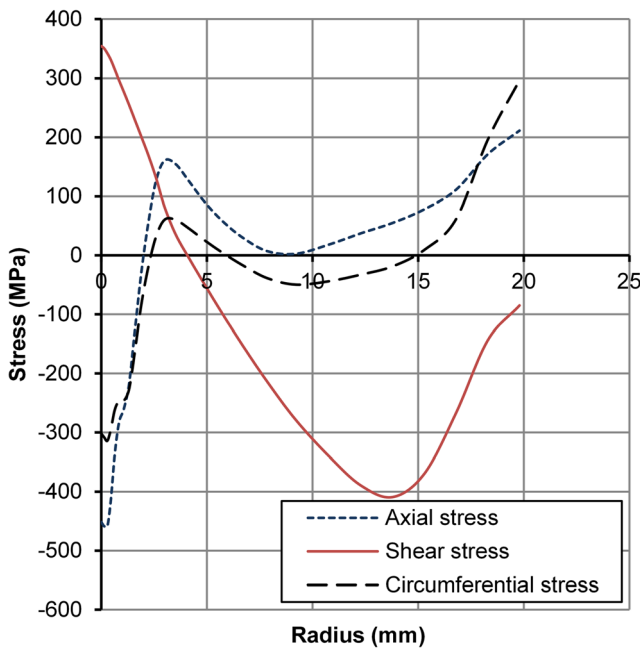

Fig. 14 Comparison of calculated residual stresses after presetting of different FE models (*torsion bar* - Type III)

Fig. 16 Residual stresses after the deep rolling and presetting operation, FE simulation (*torsion bar* - Type I)

Fig. 18 Residual stresses after the sequence of the presetting and the deep rolling operation, FE simulation (*torsion bar* - Type III)

the sequence of presetting and the deep rolling operation is shown in Fig. 18.

To overcome this problem, it is possible to repeat the presetting operation. After the first presetting operation, the torsion bar material is overstrained - hardened. Due to increased yield stress of hardened material, the second presetting does not need to be conducted with the same amount of strain – twist angle as the first presetting operation (Table 1 and Fig. 13). The torsion bar can be preset with a lower value of
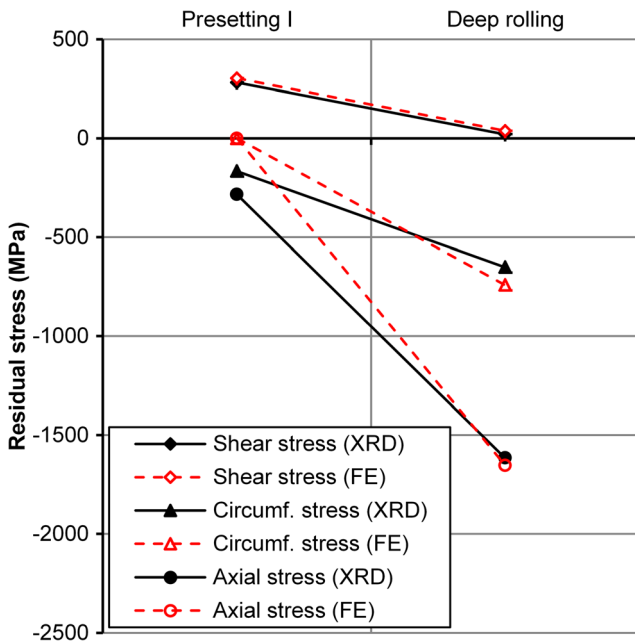

Fig. 17 Comparison of residual stresses after the first presetting and deep rolling operation (*torsion bar* - Type III)
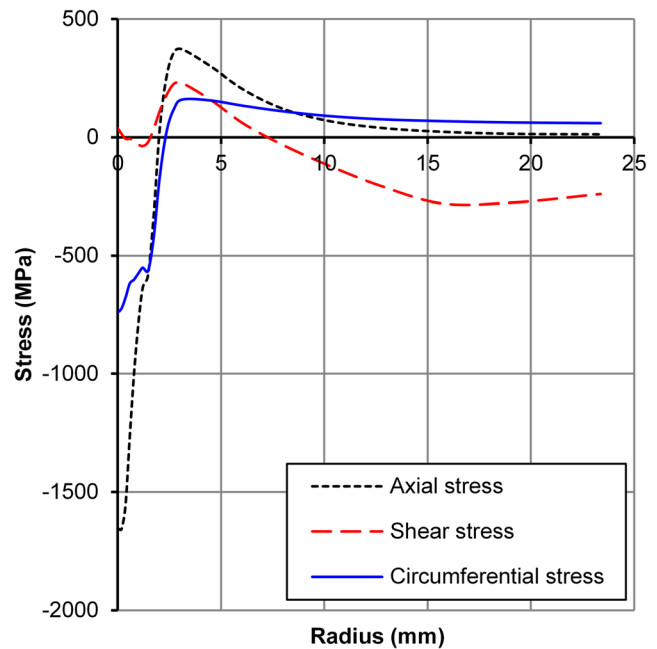
the twist angle. Presetting with a lower twist angle will obliterate stresses in axial and circumferential direction, but this effect will be smaller as evident from Fig. 19.

The obliteration effect of residual stresses after the second presetting operation with a smaller twist angle will be lower. The level of axial and circumferential residual stresses will be higher. A higher level of residual stresses is beneficial for fatigue life of the torsion bar.

Operation of the deep rolling includes a relative movement of the roller and the workpiece. It means that the torsion bar can be deep rolled in the clockwise and counterclockwise direction. The presetting operation is also conducted in both directions, which depends on the service load direction of the torsion bar. The residual stresses level is influenced by the deep rolling and presetting direction (Fig. 20).

If the direction of deep rolling is in the opposite direction of presetting, the residual stresses will be lower. This difference is not significant, but as we would like to have higher residual stresses at the surface, it is better to preset the torsion bar in the same direction as it was deep rolled.

Conclusions

In the production process of torsion bars, two specific production operations were used: deep rolling and presetting. Both operations induce favorable residual stresses in the torsion bar. Residual stresses have a major impact on fatigue life and load strength of the torsion bar. The deep rolling operation induces compressive

Fig. 19 Residual stresses after the sequence of the first presetting, deep rolling and second presetting operation (*torsion bar* Type III)
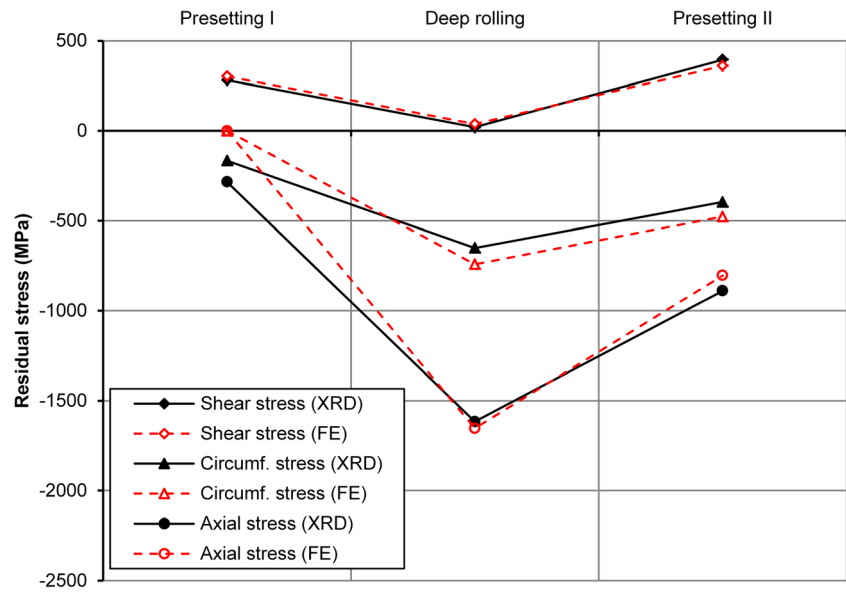
residual stresses into subsurface regions of the torsion bar. These high residual compressive stresses prevent initiation and growth of surface cracks. During the presetting operation, the torsion bar is overstrained and hardened. The results of the presetting operation are induced residual shear stresses and higher yield stress of the material. In this manner, the loading strength of the torsion bar is increased.

In this article, the production sequence of the deep rolling and the presetting operations were simulated. Different combinations of specific production sequences were simulated
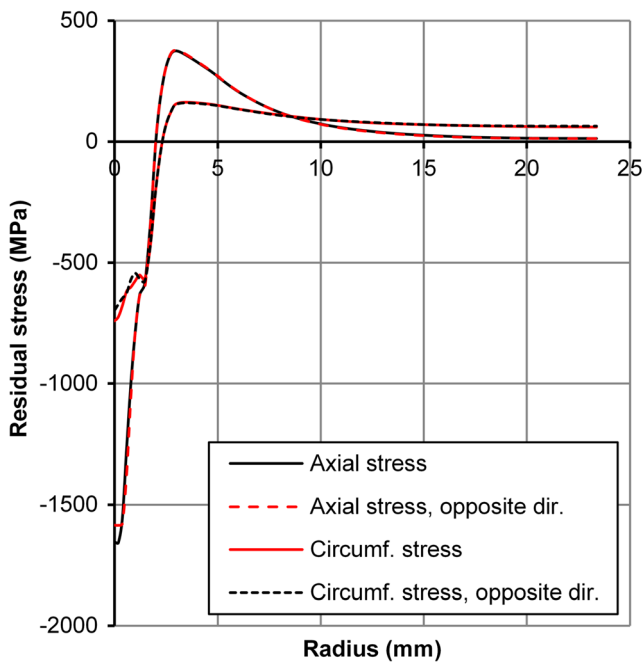

Fig. 20 Simulation of residual stresses after the sequence of the first presetting and deep rolling in the same and opposite direction

with the use of mapping functionality and FE simulation of a representative cut-out model. The results of FE simulations were verified with the measured residual stresses. From the obtained results, the following can be concluded:

- The presetting operation obliterates residual stresses induced previously by the deep rolling operation. The level of the final residual stresses depends on the technology parameters of the presetting and the deep rolling processes. Smaller deformation during presetting means higher residual axial and circumferential stresses at the end of the deep rolling – presetting sequence.

- The deep rolling operation after the presetting of the torsion bar obliterates shear stresses induced during the presetting operation. The final level of shear stresses affects the load strength of the torsion bar. If deep rolling is the last operation of the production sequence of the torsion bar, the torsion bar can sustain lower service loads compared to the torsion bar that was deep rolled before being preset.

- The second presetting operation after the first presetting and deep rolling process will increase the level of residual shear stresses. Furthermore, if it is done with the appropriate technology parameter, that is a smaller twist angle than in the first presetting operation, the influence on residual stresses after deep rolling will be smaller. Thus higher residual stresses will be presented in the torsion bar at the end of the production sequence.

- The direction of the deep rolling and presetting operations also influences the level of residual stresses. If the torsion bar is preset in the same direction as it was deep rolled, the residual stresses will be higher.

References

1. Almen J (1951) Torsional Fatigue Failures. Prod Eng 22:167–182
2. Swift W a C (1976) On the scragging of circular section bars and tubes. J Strain Anal Eng Des 11:69–77. doi:10.1243/03093247V112069
3. Eerden RL Van, Cambell K, Holly ML, et al. (2000) Manual on Design and Manufacture of Torsion Bar Springs and Stabilizer Bars, SAE HS-796. SAE International
4. Altenberger I, Scholtes B, Martin U, Oettel H (1999) Cyclic deformation and near surface microstructures of shot peened or deep rolled austenitic stainless steel AISI 304. Mater Sci Eng A 264:1–16. doi:10.1016/S0921-5093(98)01121-6
5. Schulze V (2006) Modern mechanical surface treatment. Wiley-VCH Verlag GmbH & Co., Weinheim
6. Swift W a C (1978) On the measurement of residual shear stress in scragged torsion bars. J Strain Anal Eng Des 13:157–163. doi:10.1243/03093247V133157
7. Fujczak R (1991) Correlation between Machine Twist Angle and Unit Twist Angle in Calculating Shear Stresses for Elastic and Plastic Strains in Torsion
8. Kim HS (2001) Finite element analysis of torsional deformation. Mater Sci Eng A 299:305–308. doi:10.1016/S0921-5093(00)01416-7
9. Brabie G (2003) An analysis of the shearing stresses distribution on the cross-section of the twisted round bars. J Mater Process Technol 142:224–230. doi:10.1016/S0924-0136(03)00584-3
10. Rees DW a (2009) Descriptions of reversed yielding of a solid circular bar in torsion. Proc Inst Mech Eng Part C J Mech Eng Sci 223:557–571. doi:10.1243/09544062JMES919
11. Wang H, Rui Q, He X (2007) The prediction technology study of fatigue life for key parts of a tracked vehicle's suspension system. Front Mech Eng China 2:68–71. doi:10.1007/s11465-007-0011-0
12. Skalski K, Morawski A, Przybylski W (1995) Analysis of contact elastic–plastic strains during the process of burnishing. Int J Mech 37:461–472
13. Guagliano M, Vergani L (1995) Residual stresses induced by deep rolling in notched components. Trans Eng Sci 8:109–119
14. Mayer HM, Achmus C, Pyzalla A (2000) Increase of fatigue strength of crankshafts by deep-rolling and induction hardening induced beneficial residual stress states - experimental determination and FEM simulation. Mater Week 2000:1–9
15. Demurger J, Forestier R, Kieber B, Lasne P (2006) Deep rolling process simulation: impact of kinematic hardening on residual stresses. Proc ESAFORM 1–5
16. Majzoobi GH, Azadikhah K, Nemati J (2009) The effects of deep rolling and shot peening on fretting fatigue resistance of Aluminum-7075-T6. Mater Sci Eng A 516:235–247. doi:10.1016/j.msea.2009.03.020
17. Bäcker V, Klocke F, Wegner H et al (2010) Analysis of the deep rolling process on turbine blades using the FEM/BEM-coupling. IOP Conf Ser Mater Sci Eng 10:1–10. doi:10.1088/1757-899X/10/1/012134
18. Manouchehrifar A, Alasvand K (2012) Finite element simulation of deep rolling and evaluate the influence of parameters on residual stress. 5th WSEAS Int. Conf. Cambridge, pp 61–67
19. Balland P, Tabourot L, Degre F, Moreau V (2013) An investigation of the mechanics of roller burnishing through finite element simulation and experiments. Int J Mach Tools Manuf 65:29–36. doi:10.1016/j.ijmachtools.2012.09.002
20. Trauth D, Klocke F, Mattfeld P, Klink A (2013) Time-efficient Prediction of the Surface Layer State after Deep Rolling using Similarity Mechanics Approach. Procedia CIRP 9:29–34. doi:10.1016/j.procir.2013.06.163
21. Werke M (2009) Simulation of manufacturing sequences for verification of product properties. KTH, Stockholm
22. Afazov S (2009) Simulation of manufacturing processes and manufacturing chains using finite element techniques. The University of Nottingham
23. Altenberger I (2005) Deep Rolling—The Past, the Present and the Future. Proc 9th Int Conf Shot Peen 144–155
24. Klocke F, Bäcker V, Wegner H (2009) Influence of process and geometry parameters on the surface layer state after roller burnishing of IN718. Proc Natl Acad Sci U S A. doi:10.1007/s1
25. Klocke F, Shirobokov A, Mattfeld P, Feuerhack A (2014) Festwalzen von Feinschneidstempeln. Werkstattstechnik 104:660–665
26. Chaboche JL (2008) A review of some plasticity and viscoplasticity constitutive theories. Int J Plast 24:1642–1693. doi:10.1016/j.ijplas.2008.03.009
27. Lemaitre J, Chaboche J (1990) Mechanics of solid materials. Cambridge University Press, New York
28. Kunc R, Prebil I (2003) Low-cycle fatigue properties of steel 42CrMo4. Mater Sci Eng A 345:278–285. doi:10.1016/S0921-5093(02)00464-1
29. Yang M, Akiyama Y, Sasaki T (2004) Evaluation of change in material properties due to plastic deformation. J Mater Process Technol 151:232–236. doi:10.1016/j.jmatprotec.2004.04.114
30. Sun G-Q, Shang D-G (2010) Prediction of fatigue lifetime under multiaxial cyclic loading using finite element analysis. Mater Des 31:126–133. doi:10.1016/j.matdes.2009.06.046
31. Nalla R, Altenberger I, Noster U et al (2003) On the influence of mechanical surface treatments—deep rolling and laser shock peening—on the fatigue behavior of Ti–6Al–4 V at ambient and elevated temperatures. Mater Sci Eng A 355:216–230. doi:10.1016/S0921-5093(03)00069-8